NASA

Technical Memorandum 78106

The Diffuse Component of The Cosmic X-Radiation

E. A. Boldt

MARCH 1978

National Aeronautics and
Space Administration

Goddard Space Flight Center
Greenbelt, Maryland 20771

THE DIFFUSE COMPONENT OF THE COSMIC X-RADIATION

(A transcription of a talk presented in the session "First Results From HEAO-1" at the Annual Meeting of the American Association for the Advancement of Science, Washington, D. C. February 13, 1978)

Elihu Boldt

Laboratory for High Energy Astrophysics
NASA/Goddard Space Flight Center
Greenbelt, Maryland 20771

ABSTRACT

The A-2 experiment* on HEAO-1 is the first specifically developed to study the diffuse radiation of the entire X-ray sky over a wide bandwidth, covering both the soft X-ray emission from nearby regions of the galaxy and the isotropic hard X-radiation indicative of remote extragalactic origins. A picture that is emerging from this study is that a hot thermal plasma, on a scale comparable to that of the universe, may be the principal source of hard X-radiation characteristic of the extragalactic sky. Defining some key features of this background is a prime goal of this experiment, and work in progress on this is described.

Subject Headings: extragalactic sources--X-rays, background--X-rays, spectra

*Principal investigators are E. Boldt, NASA/Goddard Space Flight Center, Greenbelt, Maryland and G. Garmire, California Institute of Technology, Pasadena, California.

The X-ray sky is dominated by an apparently diffuse flux. For soft X-rays (i.e. wavelengths $\gtrsim$ 40 Å, photon energies $\lesssim$ 0.3 keV) the anisotropies are most pronounced, associated mainly with nearby regions of our Milky Way galaxy. For hard X-rays (i.e. wavelengths < 4 Å, photon energies > 3 keV) the sky background is remarkably isotropic, indicative of extragalactic origins that are extremely remote. The HEAO A-2 experiment is now performing an all-sky survey over a broad bandwidth of photon energies (0.15 - 60 keV) that spans these two very different regimes, thereby providing the kind of information needed for studying both the galactic and extragalactic components with related observations extending well into the region of overlap. Two groups are collaborating on this extensive research program. One of these is our group (see Table 1a) at the Goddard Space Flight Center, where the principal effort is concerned with the hard X-ray data. The other group involving astronomers at the California Institute of Technology and the University of California (see Table 1b), headed by G. Garmire of Caltech, has been most interested in soft X-rays and is leading the HEAO work in that area. In this talk I will emphasize the hard component of the diffuse X-ray background.

The soft and hard X-ray regimes tend to distinguish galactic from extragalactic effects mainly because of the vastly different thermal settings for the astronomical plasmas involved. Within the galaxy, supernovae and stellar winds contribute to a million or so degree hot gas that fills a substantial fraction of the region between stars. The presence of this hot gas is important for the dynamics of the cooler

TABLE 1

a) Analysis of Hard X-rays (1.5 - 60 keV)

-- Goddard Space Flight Center:

R. Becker*
E. Boldt
S. Holt
L. Kuzienski*
F. Marshall
R. Miller+++
R. Mushotzky**
S. Pravdo*
A. Rose**
R. Rothschild+
J. Saba*
P. Serlemitsos
R. Shafer*
B. Smith**
A. Stottlemyer++
J. Swank
A. Szymkowiak*
D. Worrall*

b) Analysis of Soft X-rays (0.15 - 3 keV)

-- California Institute of Technology
(including Jet Propulsion Laboratory):

P. Agrawal
F. Cordova
G. Garmire
F. Lamb
J. Nugent
G. Riegler
I. Tuohy

-- University of California (Berkeley):

S. Bowyer
W. Cash
P. Charles
S. Khan
M. Lampton
S. Lea
K. Mason
U. Reichert
J. Thorstensen
F. Walter

* University of Maryland
** National Research Council (resident associate)
+ Now at University of California (San Diego)
++ Computer Sciences Corp.
+++ Now at Jet Propulsion Laboratory (Caltech)

gas of the interstellar medium, which is related to the rate of star formation. A greatly improved map of the local distribution of this hot component is now being constructed from the soft X-ray data and will be reported elsewhere by G. Garmire. On a vaster scale, aggregates of galaxies are filled with a more tenuous but much hotter gas, so hot (up to $\sim 10^{8}$°K) that the atoms corresponding to the lightest elements are completely stripped of electrons, leaving essentially only the inner-shell electrons of relatively abundant iron for generating any atomic signals, and where elementary electron-proton collisions are responsible for most of the hard X-ray emission characteristic of such a plasma. As we shall see, the preliminary picture that is emerging from our current HEAO study of the overall hard X-ray background is that an even hotter thermal plasma, on a scale comparable to that of the universe, may be the dominant source. The study of such a hot gas (plasma) could reveal new information about the early phases of galaxy and cluster formation, and the early evolution of the universe.

A pre-HEAO view of the so-called "isotropic" sky background of hard X-rays and its relation to the brightest discrete objects in the sky is shown in Figure 1. The vintage of this figure is about 1970, but the information exhibited remained essentially at this stage until HEAO. What is shown here is the spectrum for the energy flux of X-ray photons at Earth as would be seen by an omnidirectional (4π) spectrometer. The curves labeled "a", "b" and the data points give a representative idea of our knowledge of the isotropic background prior to HEAO. The a curve is typical of the power laws obtained with rocket-borne proportional

counters below 20 keV; indices for the photon number spectrum were anywhere in the range 1.4 to 1.7 (e.g. see Boldt et al., 1969, and Gorenstein et al., 1969). The balloon (Bleeker and Deerenberg, 1970) and OSO-3 data (Schwartz, Hudson and Peterson, 1970) were obtained with scintillators, where the high-energy efficiency is much better but where spectral resolution and extraneous background are more severe problems. The apparent spectral change between the rocket and balloon results was also suggested by the OSO-3 data. What was missing was proportional counter data from a single experiment up through the spectral change, somewhat beyond 20 keV. The HEAO A-2 experiment was developed to meet this need.

Below a few keV the overall flux of X-rays at the orbit of Earth is always dominated by the Sun. As shown in Figure 1, however, the overall flux at higher energies is dominated by isotropic radiation, so isotropic that it must be extragalactic in origins. Another important source of X-ray flux is Sco X-1 which is, on the average, by far the brightest object in the celestial sky of variable sources. Even considering the contributions of all other discernible objects in the X-ray sky (on an average day) the total of their flux arriving to the vicinity of the solar system would fall short of that shown in Figure 1 for Sco X-1. (The Crab Nebula is also included in Figure 1 for comparison since it is the brightest stable X-ray source and the standard candle of X-ray astronomy). That the X-ray sky is dominated by an isotropic flux is practically unique in astronomy, the only other case being the millimeter band where the sky is dominated by 2.7^{o}K black-body radiation. In radio, optical and gamma-ray astronomy the galaxy accounts for most of the local flux.

Although X-ray astronomy has certainly flourished since 1970, research on the diffuse sky, particularly the hard component, has been relatively dormant. Satellite experiments since 1970 such as those on UHURU (SAS 1), Ariel 5, ANS, SAS 3 and OSO-8 have focused our attention on individually discernible sources, particularly compact objects of high astrophysical interest, such as neutron stars. However, there was also a practical reason for this restriction during the initial decade or so of X-ray astronomy with orbiting observatories. The reason is that all X-ray detectors in orbit have a significant background arising from other than the X-ray sky. Some of the extraneous causes are cosmic rays, ambient electrons, locally generated gamma rays and induced radioactivity. And, for discrete source measurements, even the "true" diffuse X-ray sky is an undesirable contamination. Hence, the standard approach has been to make the detector's field of view as small as practical and to measure the <u>increase</u> in signal as the detector scans across the discrete source of interest.

Our strategy with HEAO A-2 for extracting the diffuse flux of celestial X-rays from the overall signal is outlined in Table 2. The main points are as follows:

1) The most fundamental aspect of a diffuse flux is that it increases linearly with solid angle. Hence, we employ two fields of view per detector; one of them is always $3^{o} \times 3^{o}$ (FWHM), the dual one is $3^{o} \times 1\frac{1}{2}^{o}$ for some detectors and $3^{o} \times 6^{o}$ for others.

2) Ambient electrons can be a problem. For our high-energy gas proportional counters, the main detector is separated from the entrance

TABLE 2

EXTRACTING THE DIFFUSE X-RAY FLUX FROM THE BACKGROUND

APPROACH

CHARACTERISTIC:	UTILIZATION:
* Diffuse Flux Increases Linearly with Solid Angle	* Several Fields of View (2 per detector) Along Scan Path
* Electron Contamination Enters Detector via Collimator	* Charged Particle Veto Layer at Entrance Window * Magnetic Broom
* Photoelectric Cross-Section Strong Function of Energy	* C_3H_8, Ar, Xe Gas for Three Energy Regimes * Layer-to-Layer Attenuation vs Photon Energy
* Charged Cosmic Rays and Compton Electrons Produce Longer Ionization Paths than Lower Energy Photo-Electrons	* Multi-Anode Veto
* 30 Minute Spin Period Can Involve Wide Range of Geomagnetic Latitudes	* Observations Repeated in Detectors Offset by 6° (1/2 Minute Time Lag)

window by a charged particle veto layer (propane filled) relatively transparent to hard X-rays. For our low energy detectors this is impossible and deflection magnets are used.

3) We detect X-rays via the photoelectric effect, which is a strong function of energy. To exploit this characteristic we have three types of gas proportional counters, optimized for low, medium and high energy X-rays designated LED, MED and HED, respectively. For soft X-rays (0.15-3 keV) we use propane, for medium energy X-rays (1.5 - 15 keV) we use argon and for hard X-rays (3-60 keV) we use xenon.

4) The electrons emerging from a photo-electrically excited atom are confined to a small region near the atom; hence we employ multi-anode veto to remove more penetrating charged particle events.

5) Finally, since the scan period of HEAO involves much of the orbit around the Earth we separate spatial and temporal effects with some counters offset by only 6^{0} along the scan path.

Figure 2 is a photograph of a medium energy detector in the lab. The other detectors look about the same. X-rays enter a mechanical collimator on top, traverse a thin window and are detected in a multi-anode multi-layer argon gas proportional chamber. The dual collimator is matched to the internal multi-celled structure of the proportional chamber; odd numbered cells are aligned with the $3^{0} \times 3^{0}$ collimator, while even numbered cells are aligned with the $3^{0} \times 1\frac{1}{2}^{0}$ collimator. Figure 3 shows the dual collimator itself in greater detail in order to convey how this scheme has been implemented.

Figure 4 is an artist's conception of what the A-2 experiment looks like as incorporated into HEAO-1. To get oriented, note that the

solar panels always face the sun. The A-2 experiment itself consists of six proportional chambers, two LED's for low energies, one MED for midband coverage and three HED's for hard X-rays.

To get some idea of how this experiment scans the sky let's concentrate on any one of the six detectors and examine its scan path on the celestial sphere. This is shown in Figure 5. Every half hour this dual collimator detector scans a complete great circle on the celestrial sphere in an angular band 3^0 wide. At any instant of time it views an angular region $\pm\theta$ along the scan path with the detector half corresponding to the large field of view collimation as well as an included angular region half this size with the complimentary portion of the detector corresponding to the small field of view. Each day the spin axis moves 1^0 along the ecliptic equator so that the entire sky is scanned in 6 months.

How does the dual collimation scheme work out in practice? The in-orbit performance of HED #1 relative to this question is exhibited in Figure 6, where the effectiveness of the scheme is quite evident. The two histograms displayed give the observed population of samples sorted according to the total accepted X-ray count per telemetry major frame (i.e. 40.96s). They are classified only as regards field of view, the top histogram for counts associated with the $3^0 \times 6^0$ collimation and the bottom for counts associated with the $3^0 \times 3^0$ collimation. These histograms are based on data accumulated over many scan cycles regardless of what was in the field of view, be it the Earth or celestial sources. The histogram for each of the fields of view exhibits two clearly separated peaks, the high one attributed to exposures dominated by the sky and

the one with lower counts attributed to exposures dominated by the Earth. If there were no extraneous sources of background the two histograms would scale as the ratio of solid angles (i.e. both the Earth and the sky represent essentially isotropic sources). In fact, the Earth is a relatively weak X-ray source, even in the hard X-ray band ($\sim$ 3-60 keV) considered here, and most of the signal when the Earth fills the field of view arises from background internal to the detector (e.g. Compton collisions of gamma rays). More extensive data bear out the qualitative indication in Figure 6 that the internal background to be associated with the two fields of view are equal. Furthermore, a comparison of the internal background derived from the two peaks associated with the diffuse sky has been shown to be the same as that derived from the two peaks associated with the diffuse Earth, both in magnitude and spectral shape. As shown in Figure 6 by a dashed line, the internal background for HED #1 represents an average contamination of $\sim$14% for the large field of view and $\sim$25% for the small field of view, when the full 60 keV energy bandwidth of this detector is included.

At this point we felt ready to start our analysis of the spectrum of the diffuse X-ray background. The work I'll be describing on this was carried out as a pilot study by F. Marshall with some key inputs from R. Miller. In this instance, we excluded much of the available data because of criteria such as 1) no catalogued source or source region in the field of view, 3) no transient activity or new source, down to a level of less than 2×10^{-3} Crab* and, of course, 3) none of the Earth in the field of view. To exclude effects of internal background,

*Note that a "milliCrab" is approximately equivalent to one UHURU count/s.

the pulse height spectrum to be associated with the diffuse background was obtained in each detector by simply subtracting the spectrum for the small field of view from the spectrum for the large field of view. Then we tested some model spectra of interest by folding them through the calibrated response function of the detector, normalizing to the total number of counts and comparing observed counts per channel with that predicted. The response function for this procedure was verified, in orbit, on the Crab Nebula. For the diffuse background, we considered two power-law spectra of interest (i.e., photon number index 1.4 and 1.7) and the results are shown in Figure 7.

The quantity plotted in Figure 7 is the ratio of observed to predicted counts as a function of observed energy (in keV). Because of the decreasing photon flux and detector efficiency with energy the statistical errors increase with energy. Below about 20 keV these errors are smaller than the symbols used for the data points but become appreciable above about 40 keV, as shown by the error bar on the bottom plot in the figure. From the top plot of Figure 7 we see that the incident spectrum definitely falls off more rapidly than a 1.4 power-law above about 10 keV. From the bottom plot, we see that although a 1.7 index power-law might represent a better overall fit qualitatively, it is also clearly not acceptable.

We then tried spectra corresponding to the emission expected from an optically thin hot isothermal plasma of electrons and protons. This was tried for several temperatures, as shown in Figure 8. Here again we plot the ratio of observed to predicted counts. As is evident, kT = 20 keV is much too cool while kT = 75 keV is definitely too hot. At

this stage of data analysis we estimate that kT is within about 5 keV of 45 keV. In other words, the temperature is about a half billion degrees, and the spectrum is remarkably structureless, at least below about 20 keV. For the absolute magnitude of the flux, we agree quite well with estimates by D. Schwartz (1975) based on a compilation of pre-HEAO measurements by various experiments over different portions of the spectrum.

Now let's compare this background spectrum with the spectra of specific extragalactic objects. Most of those so far identified are clusters of galaxies (McHardy, 1977; Jones and Forman, 1978); the brightest extragalactic X-ray object in the sky is the Perseus Cluster. It's spectrum is also thermal and is shown in Figure 9, based on data obtained by P. Serlemitsos, R. Mushotzky, B. Smith and colleagues from our OSO-8 experiment. The list of 20 such spectra now known (Mushotzky et al. 1978) should increase to about 60 when we complete the HEAO analysis of clusters from an all-sky survey. In this case, the thermal emission is characterized by kT = 6.8 keV for the continuum and an equivalent width of 400 eV for a line at 6.7 keV indicative of a near cosmic abundance of iron in collisional equilibrium this temperature. These are reasonably typical parameters for X-ray clusters. In other words, they are much cooler than the overall background, and they do have spectral structure.

The next most common extragalactic X-ray source identified prior to HEAO is a Seyfert galaxy. Although there are about 14 (Elvis et al. 1978) we knew the spectrum of only one, namely NGC4151. Figure 10 shows another one, obtained from our HEAO experiment by R. Mushotzky,

for an object with an intensity of less than 10^{-3} Crab. This extreme Seyfert N-galaxy 3C390.3 was in a low state during the accumulation of these data. The incident spectrum inferred is based on a best-fit power law of number index 1.7 and absorption by 5 x 10^{22} atoms cm^{-2}, roughly equivalent in magnitude to the absorption between here and our own galactic center. In summary, it's not a thermal spectrum and it is highly absorbed, such as NGC4151.

As far as other compact extragalactic sources, there were spectra for only two prior to HEAO (i.e., the quasar 3C273 and the BL Lac object Markarian 421). Now that the A1 and A3 experiments have identified another BL Lac object (Markarian 501), here is another BL Lac spectrum obtained from the A2 experiment by R. Mushotzky, shown in Figure 11. It is a remarkably flat spectrum, much like that of Markarian 421 (R. Mushotzky, private communication), with a photon number spectral index of 1.1 and exhibits no apparent absorption.

We are now in a position to compare the various major components of the extragalactic hard X-ray sky. First, we have the spectrum of the diffuse background (i.e., the spectrum for the composite emission of all unresolved sources). For resolved sources we already have a good idea of the typical spectrum to be associated with clusters of galaxies. As we have just seen we also have some idea of the highly absorbed spectra to be associated with relatively compact objects such as Seyferts and N-galaxies to the very flat unabsorbed spectra to be associated BL Lac objects such as Markarian 501. For previous surveys such as conducted with UHURU and Ariel 5 we know the identity of over 80% of the extragalactic

sources resolved and we know how the number of such objects decreases with source intensity over about a decade; that is, we know something about the so-called Log N-Log S curve for observations in the 2-10 keV band (Murray 1977; Warwick and Pye, 1978). Hence, we have what we need to construct the spectrum for the composite flux from almost all extragalactic sources that could have been resolved prior to HEAO. This information is summarized in Figure 12.

Figure 12 shows the spectral characteristics of the total flux from the extragalactic X-ray sky as would be viewed by an omnidirectional (4π) spectrometer. The curve labeled "unresolved emission" is the best fit thermal continuum for the diffuse background; as discussed before, this corresponds to kT $\gtrsim$ 45 keV. The curve labeled "clusters of galaxies" represents a thermal continuum with kT $\gtrsim$ 6 keV and iron line emission at $\sim$ 6.7 keV spread out in energy over a bandwidth corresponding to a spread in redshifts of 0.09 since the most distant cluster with detected line emission (Abell 478) has that redshift. The curves labeled "Seyferts" and "QSO + BL Lac" are very approximate in shape since spectra have been measured for only a couple of sources in each instance, although the absolute 2-10 keV level is based on larger samples, especially for Seyferts. From the most distant source of each class positively identified we can crudely estimate what the multiplication factor is for getting from these flux values shown here to ones corresponding to the integral of all such sources in the universe. For clusters of galaxies that factor is less than about 5. For Seyferts the factor is approximately 10. For "QSO + BL Lac" the factor would be less than 10 if we really

believed we could ignore evolution for such sources. On this basis, we conclude that at no energy do discrete sources of the type indicated contribute more than about a tenth of the unresolved emission spectrum shown here, with clusters making their major contribution at the low energy end and Seyferts at the high end. In particular, the iron line emission from clusters is so pronounced that the resulting discontinuity in the unresolved emission as observed in this experiment would be close to 1%; anything much more than this would have been detected in the limited data sample already analyzed.

We are confronted with the situation that it is extremely difficult, if not impossible, to account for most of the unresolved extragalactic X-ray sky in terms of extragalactic X-ray objects like those already observed. In fact, the spectral shape suggests that it's thermal emission from a hot plasma at an effective temperature of a half-billion degrees. If it's a spatially uniform plasma, we can apply the analysis of Field and Perrenod (1977) to conclude that the mass in this plasma is about half that required for closure of the universe. However, there are serious problems with this picture, as pointed out by these authors and others (cf. Bergeron and Gunn 1977). For example, the existence of diffuse neutral hydrogen clouds in intergalactic space indicates that the hot plasma under consideration can not pervade all intergalactic space for if it did these hydrogen clouds could not persist. One way to get around this is to postulate that the intergalactic plasma is clumped. A model discussed by Field and Perrenod (1977) has this matter in isothermal spheres of a type described by Chandresekhar (1942) many years ago.

If one assumes that the total mass in such hot clouds is less than the closure mass, then the number of such objects must be less than 2×10^5 sources. However, upper limits on background fluctuations, such as obtained by Schwartz et al. (1971), Fabian and Sanford (1971) and Shafer et al. (1977), require that the number of discrete sources for the background exceed 2×10^5 objects by at least a factor of 2. However, these analyses were basically for point sources, while the hot spheres discussed by Field and Perrenod (1977) could have radii larger than 100 Mpc and present an angular size greater than a degree. That's the situation as it exists now. Defining some key characteristics of this background necessary for solving this puzzle is a major goal of our elaborate program of data analysis. Some of the topics we are pursuing are listed in Table 3. In brief, the status on these may be summarized as follows:

Topic #1. F. Marshall is leading our work on the spectrum of the background. The results presented today represent less than 5% of the data we hope to have from this mission.

Topic #2. Research on extragalactic sources with HEAO is just beginning and you've seen some examples. R. Mushotzky, B. Smith, and D. Worrall are carrying this forward.

Topic #3. For the fields of view employed by this experiment source confusion, even for extragalactic sources, is a problem at the level of $\sim 10^{-3}$ Crab and becomes very severe below 10^{-4} Crab. Yet we would like to extend our spectroscopy for extragalactic sources down to that level. To do this we ignore source confusion and measure the energy spectrum of the brightness fluctuations characteristic of the

TABLE 3

RESEARCH IN PROGRESS ON THE UNRESOLVED HARD X-RAY SKY

1. Spectrum of the isotropic (extragalactic) background.

2. Spectroscopic comparison with resolved extragalactic sources (e.g. clusters of galaxies, Seyferts).

3. Spectroscopic comparison with unresolved extragalactic sources.

4. Multicolor analysis of fluctuations in the extragalactic brightness (e.g. for classificatic of contributing components).

5. Auto-correlation analysis of fluctuations in the extragalactic brightness (i.e. scales of clumpiness).

6. Correlation analysis of variations in the extragalactic brightness (e.g. local supergalaxy).

7. Finding the proper frame for the extragalactic background (e.g. Compton-Getting effect).

8. Unresolved galactic emission due to low luminosity objects.

9. Diffuse galactic emission due to cosmic ray electrons (e.g. correlations with the galactic radio background).

extra-galactic sky in regions devoid of individually resolvable sources and compare this directly with the spectrum of the overall diffuse background. A. Stottlemyer and I have made some progress on this, but we need to analyze an order of magnitude more data to rise above the limitations of counting statistics.

Topic #4. As we saw in Figure 10, clusters of galaxies dominate the discrete source component of the extragalactic sky below $\sim$ 10 keV while Seyferts dominate above $\sim$ 10 keV. By examining the fluctuations in sky surface brightness separately for these two regimes R. Shafer will, in effect, be setting constraints on the Log N-Log S relation for these two classes of objects down to a level somewhat below 10^{-4} Crab.

Topic #5. To obtain statistically independent samples of the sky relative to point objects it is sufficient to require that there be no overlap in the fields of view. For extended objects it's more complicated. In this case R. Shafer is using an autocorrelation analysis. This is particularly important for establishing some characteristic parameters of a possibly clumpy intergalactic hot plasma.

Topic #6. We already know from the work of de Vaucouleurs (1971) and others that the local region of the universe within $\sim$ 20 Mpc is not isotropic in optically observable galaxies and that this so called "local supergalaxy" is likely to be anisotropic in X-rays as well. However. the rather pronounced fluctuations intrinsic to the X-ray sky impose a noise on such measurements of surface brightness variations that amounts to several per cent over resolution elements of a few square degrees. To get around this problem S. Pravdo is first trying a global strategy

whereby he will integrate diffuse X-ray data over supergalactic longitude as a function of supergalactic latitude. Later on he will try correlations with galaxy counts.

Topic #7. Since the proper frame of the extragalactic background is not likely to be anchored to the solar system we should be able to detect our velocity relative to this preferred frame. In particular, observers of the microwave background (cf. Smoot, Gorenstein and Muller 1977) have already detected a net velocity of $\sim$ 300 km/sec. The limitation to measuring a velocity of such magnitude in X-rays is that the corresponding anisotropy amplitude is only about 0.4% and we have relatively large fluctuations intrinsic to the sky to deal with. However, these fluctuations can be minimized by rejecting data contaminated with resolved sources. By rejecting sources at the level of 0.5 milli-Crab the ultimate sensitivity corresponds to the detection of an amplitude of 0.4% at a statistical level somewhat better than 4σ. Since we still don't know about intrinsic sky fluctuations above 10 keV, this higher energy regime is still an open question. However, for the full bandwidth of this experiment, F. Marshall has already established an upper limit of about 1% based on a small fraction of the available data.

Topic #8. Bleach et al. (1972) and Holt et al. (1974) have considered that some of the weak unidentified hard X-ray sources at high galactic latitude might represent a relatively large population of low luminosity objects within our galaxy producing a ridge of unresolved hard X-ray emission. Observations prior to HEAO by R. Bleach in our group and W. Wheaton (1976) at UCSD give some evidence for such a ridge. This

apparently diffuse hard X-ray emission is being investigated with our HEAO data. However, the real breakthrough on this question came when we began to look at some well known optical objects identified as bright, soft X-ray sources. From the work of Swank et al. (1977) we have learned that although the photon flux from AM Her is predominantly soft (at energies less than a few hundred electron units) most of the luminosity resides in hard X-rays (at energies in the tens of kilovolts range). Recently analyzed results from the ANS satellite (Heise et al., 1978) indicate that a similar situation holds for SS Cygni. We have confirmed these results and extended them with HEAO. Furthermore, after our A-2 collaborators in California (Garmire et al. 1977) discovered with HEAO that U Geminorum can also emit a huge flux of soft X-rays, J. Swank (1978, private communication) at Goddard looked carefully for a possible small flux of hard X-rays and again found that, although the flux is low, there is indeed emission in the hard X-ray band. The typical X-ray luminosity of these sources is $\sim 10^{33}$ erg/s, like the optical luminosity of our Sun, whereas most of the hundred or so hard X-ray sources in our galaxy previously detected in sky surveys have luminosities three to five orders of magnitude higher. These three low luminosity sources are all binaries, with periods in the range 3.1 - 6.5 hours, and are thought to involve accretion onto a white dwarf. These three sources are all within about 200 pc of the Sun. Sources such as these much beyond a few hundred parsecs would be unobservable in soft X-rays. However, there should be on the order of 10^4 such sources in the galaxy and, by virtue of their emission in hard X-rays, should make a major

contribution to any apparently diffuse galactic ridge seen in the hard X-ray band.

Topic #9. Finally, there should be some truly diffuse galactic X-ray background since we know that cosmic ray electrons colliding with ambient microwave photons and starlight do produce hard X-rays. Here again, as in topics #6 and #7, we must get around the problem of brightness fluctuations intrinsic to the extragalactic sky. In other words, model testing and correlations with other data are required. D. Worrall is working on this by considering models for the galactic confinement of relativistic electrons that might be tested, and she and F. Marshall a.e investigating correlations with the galactic radio background.

My coinvestigators and I thank those responsible for the beautifully performing payload that has made the A-2 experiment a suc .ss (see Table 4).

TABLE 4

PRIME RESPONSIBILITY FOR PAYLOAD (ACKNOWLEDGEMENTS)*

HEAO Project Manager	R. Browning
HEAO-1 Project Scientist	F. McDonald
A-2 Experiment Manager	D. Wrublik
Systems Engineer	R. Martin
Detector Systems	C. Glasser
Mechanical Systems	W. Sours
Gas Systems	J. Robinson
Power System	J. Westrom
Thermal System	J. Webb
Collimator Development	D. Studenick
Detector Signal Processing Electronics	C. Cancro
Data Processing Electronics	H. White
Data Format Electronics	F. Link
Electrical Control System	J. Libby
Special LED Related Systems (CIT)	J. Vu
Test Pulse Generator Design (UCB)	H. Primbsch
Electrical Integration	R. Porter
Mechanical Integration	K. Rosette
HEAO Project Manager (MSFC)	F. Speer
A-2 Experiment Manager (MSFC)	D. Talley

*At GSFC, except where indicated.

FIGURE CAPTIONS

Figure 1. The spectrum of the diffuse background omnidirectional flux (curve a) is shown with spectra for Sco X-1 and the Crab Nebula obtained with the same rocket-borne proportional counters (Boldt et al. 1969; Holt et al 1969). The spectrum for the quiet sun (Chodil et al. 1965) is shown as a dashed line. The spectrum of the diffuse background obtained with balloon-borne detectors flown by the University of Leiden (Bleeker and Deerenberg 1970) is shown as curve b. Data points shown for the background spectrum were obtained with the UCSD scintillator experiment aboard OSO-3 (Schwartz, Hudson and Peterson 1970). The solid curves indicate "best fits" to the rocket and balloon data.

Figure 2. Laboratory photograph of a medium energy detector (MED); overall length is about one meter. The copper-shielded aluminum housing is filled with P10 (argon methane mixture) proportional counter gas. The analog electronics for the detector are mounted at one end and the digital electronics are suspended below. The cylinders on the side house the drive mechanism for a calibration source that can be brought into and out of the field of view.

Figure 3. Dual collimator for MED showing $3^{o} \times 3^{o}$ and $3^{o} \times 1\frac{1}{2}^{o}$ cell arrangement, as viewed from below, on axis.

Figure 4. Artistic conception of the A-2 experiment as incorporated into HEAO-1. Starting from the side away from the Sun,

the detectors are LED #1 followed by LED #2 offset from the deck by 6^{o} (both these low energy detectors have acoustic covers which were closed during the launch and acquisition phases; they now serve as sun shields). HED #1 is next, also offset by 6^{o}, followed by HED #2 on the deck with the same collimation as HED #1. The MED is next on the deck, followed by HED #3 (closest to the solar panels) with the same collimation as the MED. The three HED's and MED have rigid sun shades, as shown.

Figure 5. A schematic representation of the celestial scan executed by any one of the six detectors of the A2 experiment. The z direction points from HEAO to the sun and provides the axis of scanning. $\theta = 1\frac{1}{2}^{o}$ for LED #1, MED and HED #3. $\theta = 3^{o}$ for LED #2, HED #1 and HED #2.

Figure 6. Histograms of observed samples sorted according to count per telemetry major frame (40.96s) for HED #1, classified according to field of view, $3^{o} \times 6^{o}$ or $3^{o} \times 3^{o}$.

Figure 7. The ratio (R) of observed to predicted counts as a function of observed energy (keV). The solid circles refer to data from the first layer of HED #1 (here designated #1) and the open circles to data from the first layer of HED #3 (here designated #3). The assumed incident spectra are of the form: $\frac{dN}{dE} \propto E^{-\Gamma}$.

Figure 8. The ratio (R) of observed to predicted counts as a function of observed energy (keV). For HED's (here designated #1 and #3) data from both layers are exhibited; layer #1 is designated M1 and layer #2 is designated M2. MED data are also used for the "best fit" spectrum, shown by X's in the middle plot. The assumed incident spectra are of the form $\frac{dN}{dE} \propto E^{-1}\, g(E,T) \exp(-E/kT)$, where g(E,T) is the Gaunt factor discussed by Matzler et al. (1977).

Figure 9. Incident photon number spectrum for the Perseus Cluster inferred from data obtained with GSFC Cosmic X-ray Spectr y experiment aboard OSO-8 (Mushotzky et al. 1978). The spectrum is unfolded from the data on the basis of a model of thermal bremsstrahlung (with iron line emission).

Figure 10. Incident photon number spectrum for 3C390.3 inferred from data obtained with HED #3 from the A2 experiment aboard HEAO-1. The spectrum is unfolded from the data on the basis of a power-law spectrum absorbed by cool matter of cosmic abundance.

Figure 11. Incident photon number spectrum for Markarian 501 inferred from data obtained with HED #1 from the A2 experiment aboard HEAO-1. The spectrum is unfolded from the data on the basis of a power-law spectrum.

Figure 12. The X-ray flux from the extragalactic sky as it would be viewed by an omnidirectional (4π) spectrometer (see text).

REFERENCES

Bergeron, J., and Gunn, J. 1977. Ap. J. 217, 892.

Bleach, R., Boldt, E., Holt, S., Schwartz, D. and Serlemitsos, P. 1972. Ap. J. (Letters) 174, L101

Boldt, E., Desai, U., Holt, S., and Serlemitsos, P., 1969. Nature 224 677; Ap. J. 156, 427.

Chandresekhar, S. 1942. Principles of Stellar Dynamics (Chicago: University of Chicago Press), p. 231.

Chodil, G., Jopson, R., Mark, H., Seward, F. and Swift, C. 1965. Phys. Rev. Lett. 15, 605.

Elvis, M., Maccaro, T., Wilson, A., Ward, M., Penston, M., Fosbury, R. and Perola, G. 1978. Mon. Not. R. Astr. Soc., in press.

Fabian A. and Sanford, P. 1971. Nature Phys. Sci. 234, 20.

Field G. and Perrenod, S. 1977. Ap. J. 215, 717.

Garmire, G., Charles, P., Mason, R., Bowyer, S., Riegler, G., Tuohy, I., Boldt, E., Holt, S., Rothschild, R. and Serlemitsos, P. 1977. IAU Circ. No. 3125.

Gorenstein, P., Kellogg, E. and Gursky, H. 1969. Ap. J. 156, 315.

Heise, J., Mewe, R., Brinkman, A. C., Gronenschild, E.H.B.M., den Roggende, A.J.F., Schrijrer, J., Parsignault, D. R. and Grindley, J.E. 1978. Astron. Astrophys. 63, L1.

Holt, S., Boldt, E. and Serlemitsos, P. 1969. ap. J. (Letters) 158, L155.

Holt, S., Boldt, E., Serlemitsos, P., Murray, S., Giacconi, R., Kellogg, E. and Matilsky, 1974. Ap. J. (Letters) 188, L97.

Jones, C. and Forman, W. 1977. Center for Astrophysics, preprint.

Matzler, C., Bai, T., Crannel, C., and Frost, R. 1977. GSFC X-660-77-203.

McHardy, I. 1977, University of Leicester, preprint.

Murray, S. S. 1977. Center for Astrophysics, preprint No. 680.

Mushotzky, R., Serlemitsos, P., Smith, B., Boldt, E. and Holt, S. 1978. Ap. J., in press.

Schwartz, D., Hudson, H. and Peterson, L. 1970. Ap. J. 162, 431.

Schwartz, D., Boldt, E., Holt, S., Serlemitsos, P. and Bleach, R. 1971. Nature Phys. Sci. 233, 110.

Schwartz, D. 1975. In X-rays in Space, ed. D. Venkatesan (Calgary: University of Calgary), p. 1096.

Shafer, R., Boldt, E., Holt, S. and Serlemitsos, P. 1977. Bull. AAS 9, 616.

Smoot, G., Gorenstein, M. and Muller, R. 1977. Phys. Rev. Lett. 39, 898.

Swank, J., Lampton, M., Boldt, E., Holt, S. and Serlemitsos, P. 1977. Ap. J. (Letters) 216, L71.

Vaucouleurs, G. de. 1971. Pub. A.S.P. 83, 113.

Warwick, R. and Pye, J. 1978. Mon. Not. R. Astr. Soc., in press.

Wheaton, W. 1976. Ph.D. Dissertation, U. Calif. (San Diego).

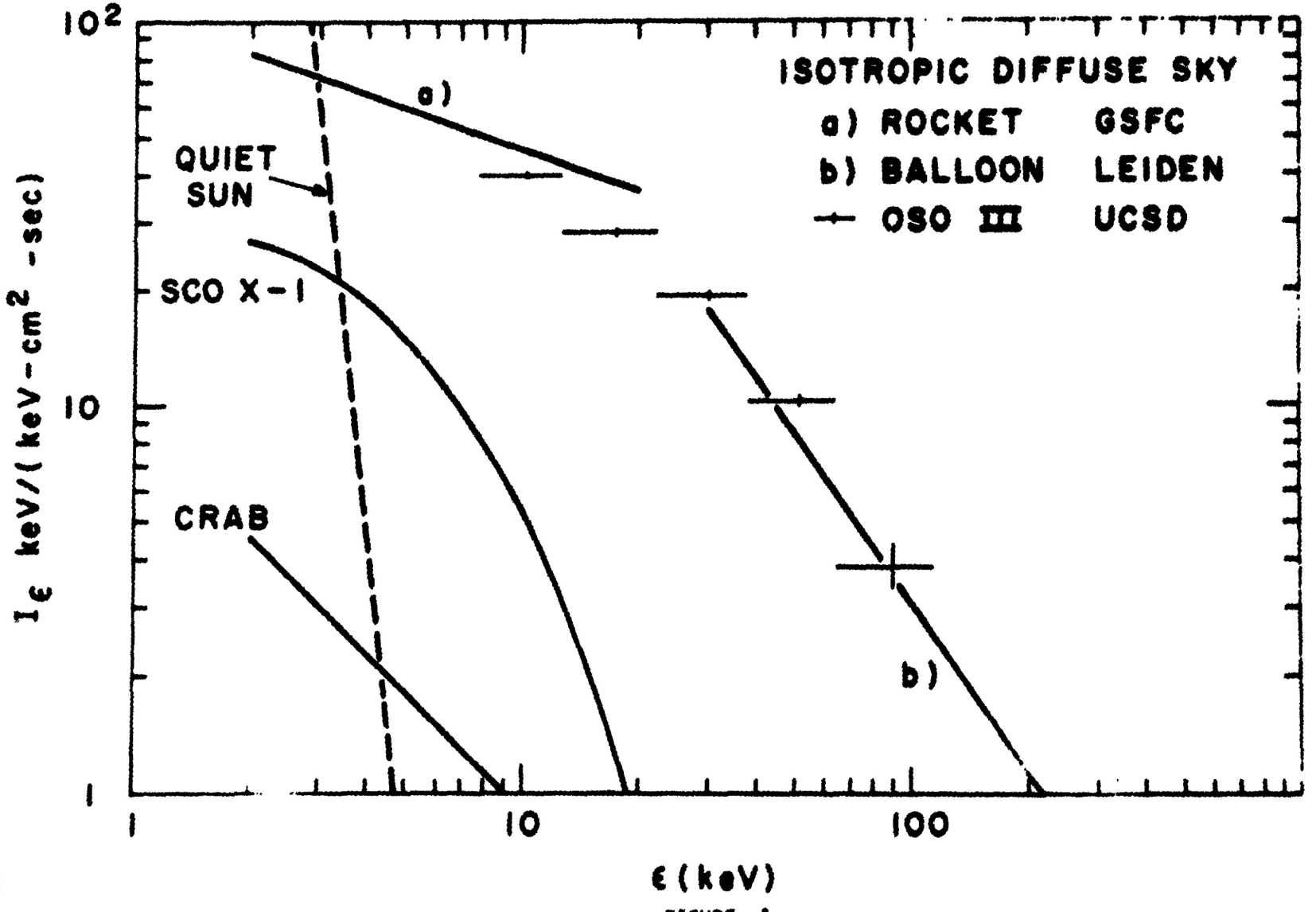

FIGURE 1

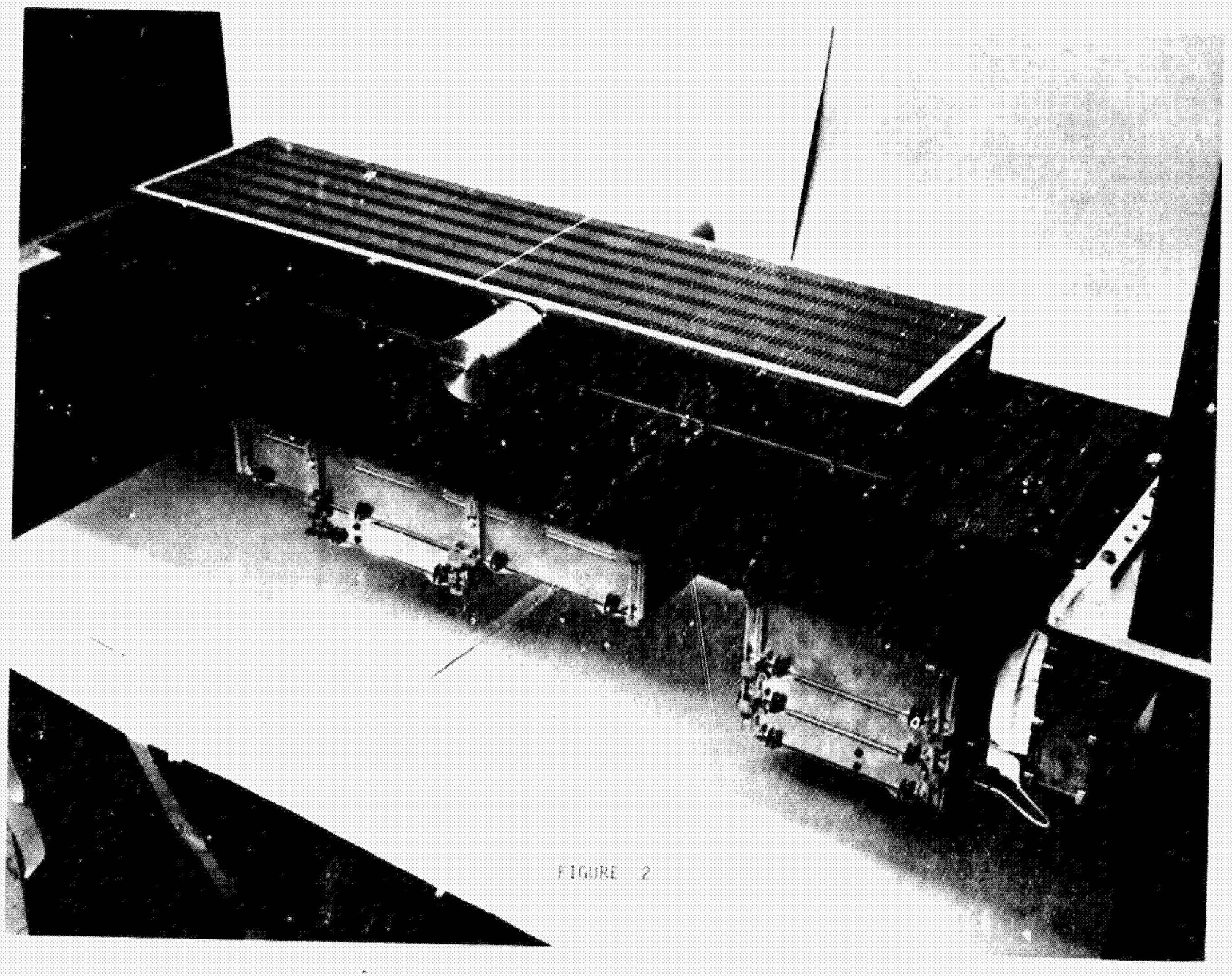

FIGURE 2

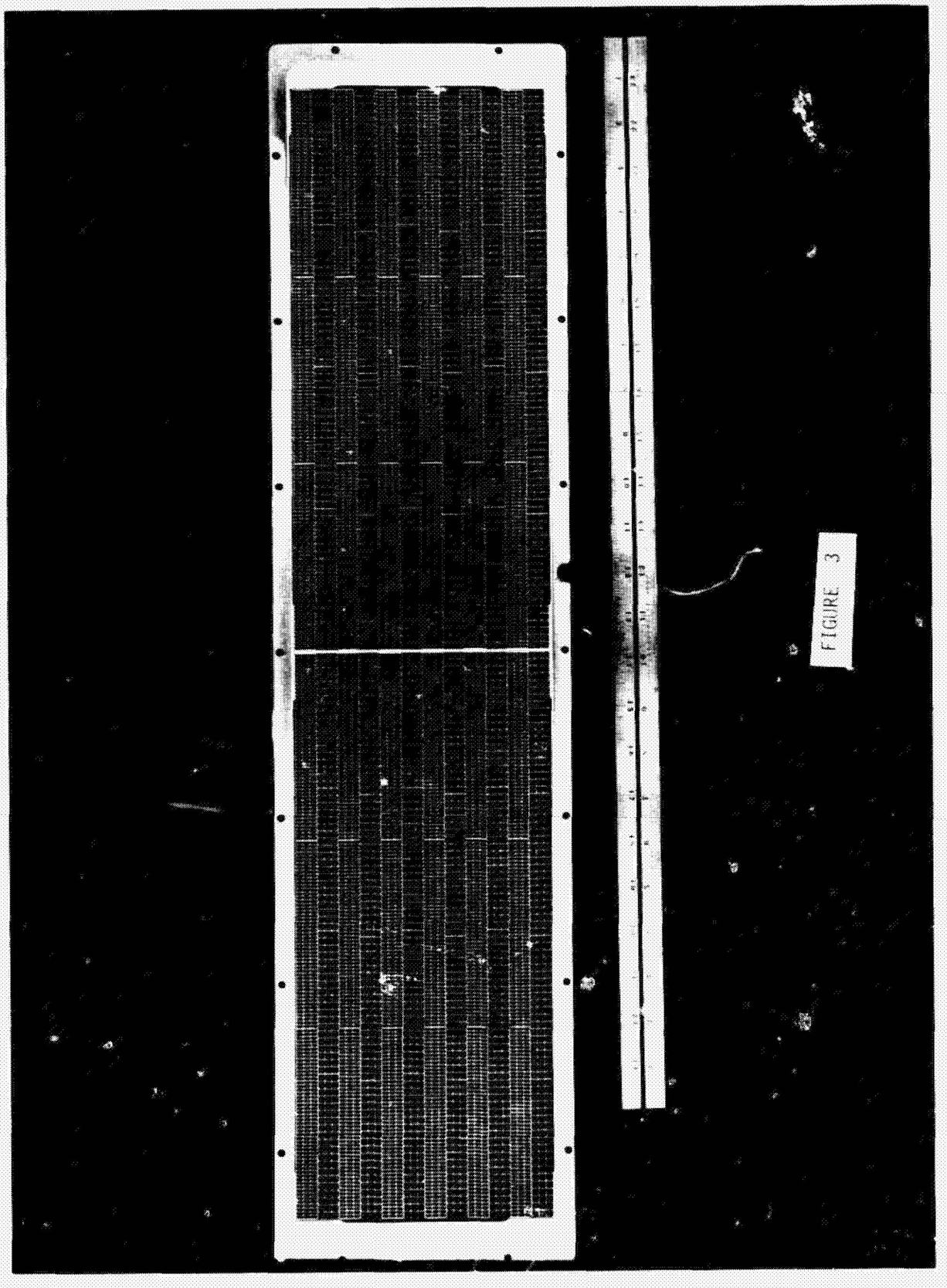

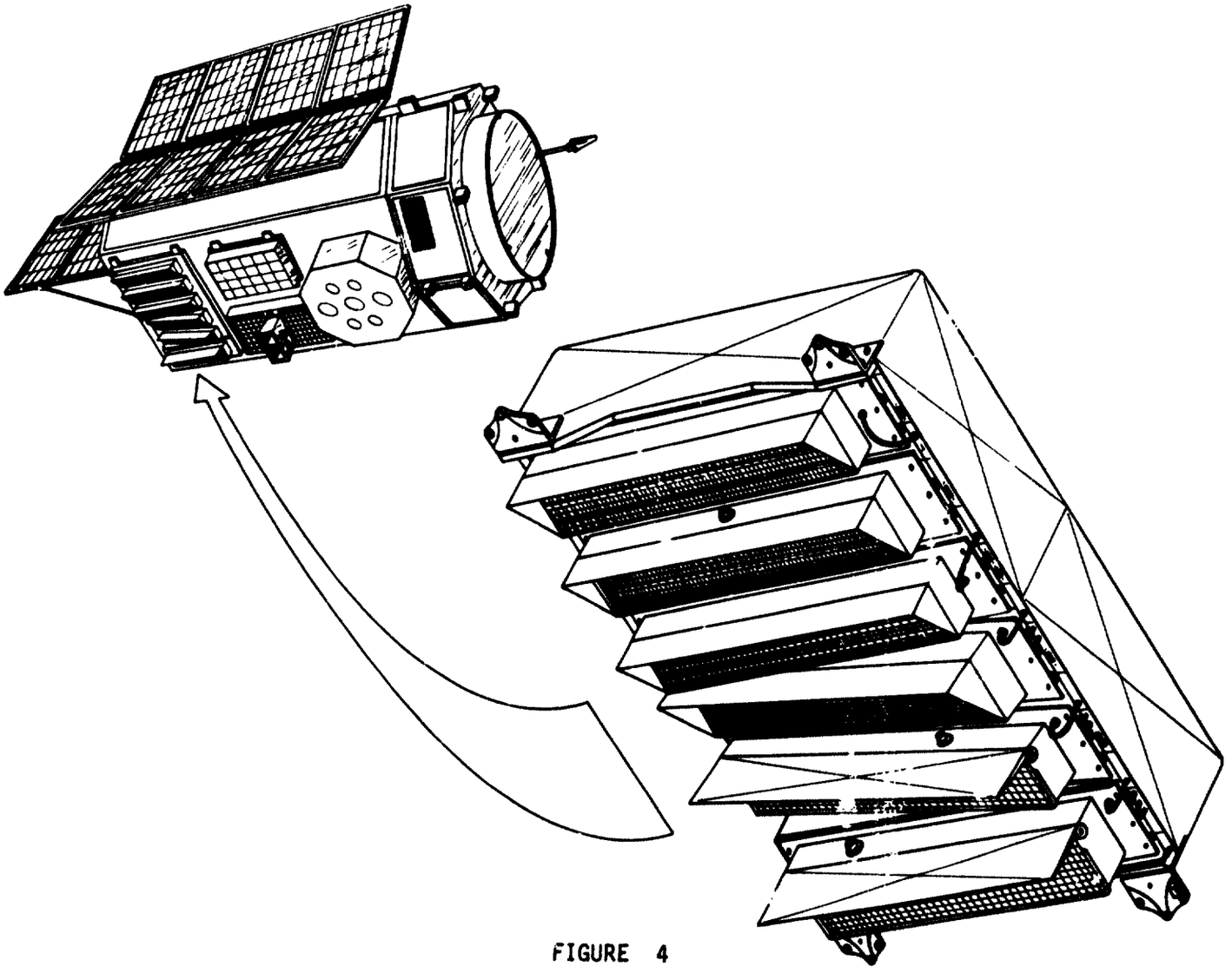

FIGURE 4

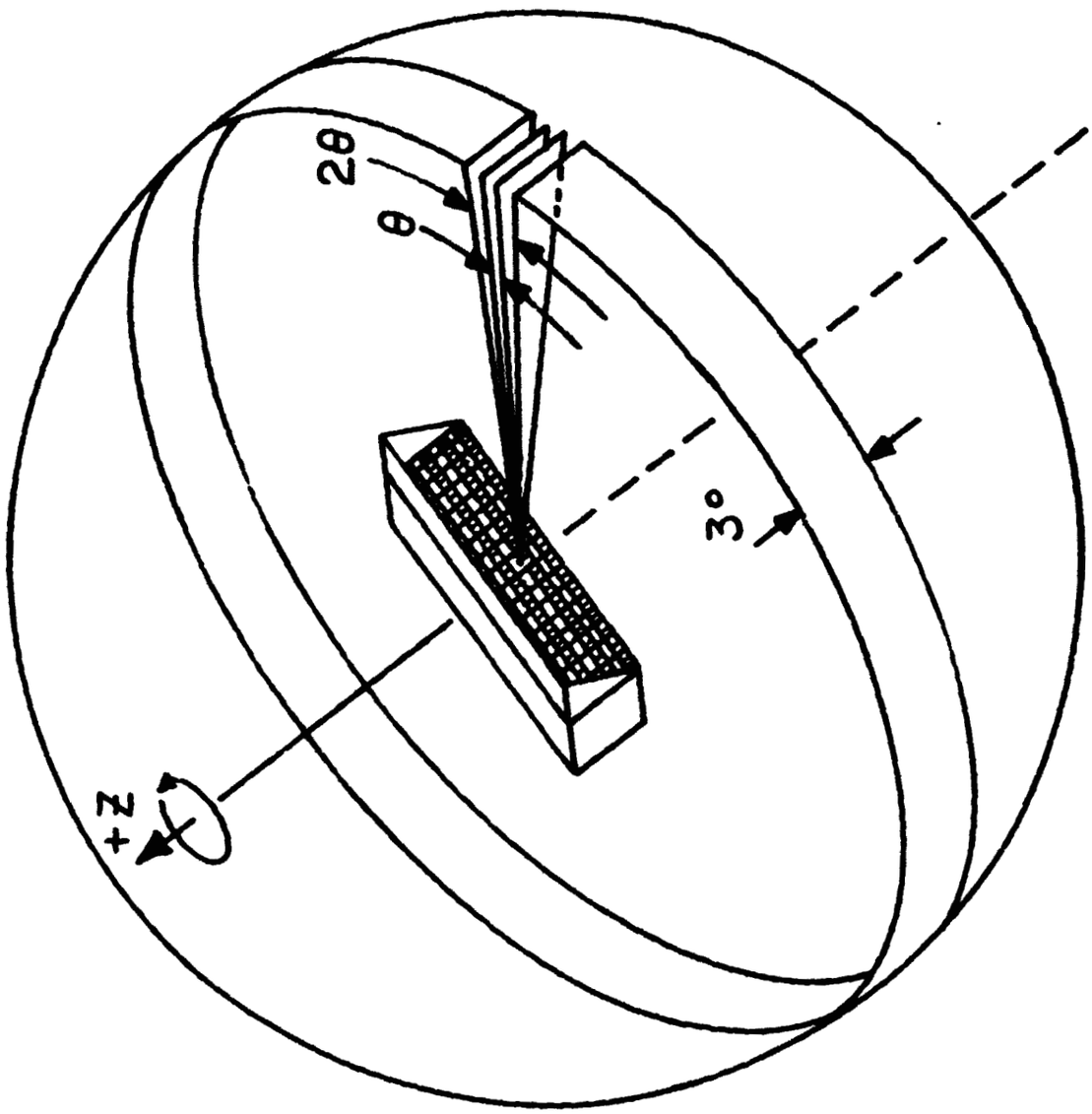

FIGURE 5

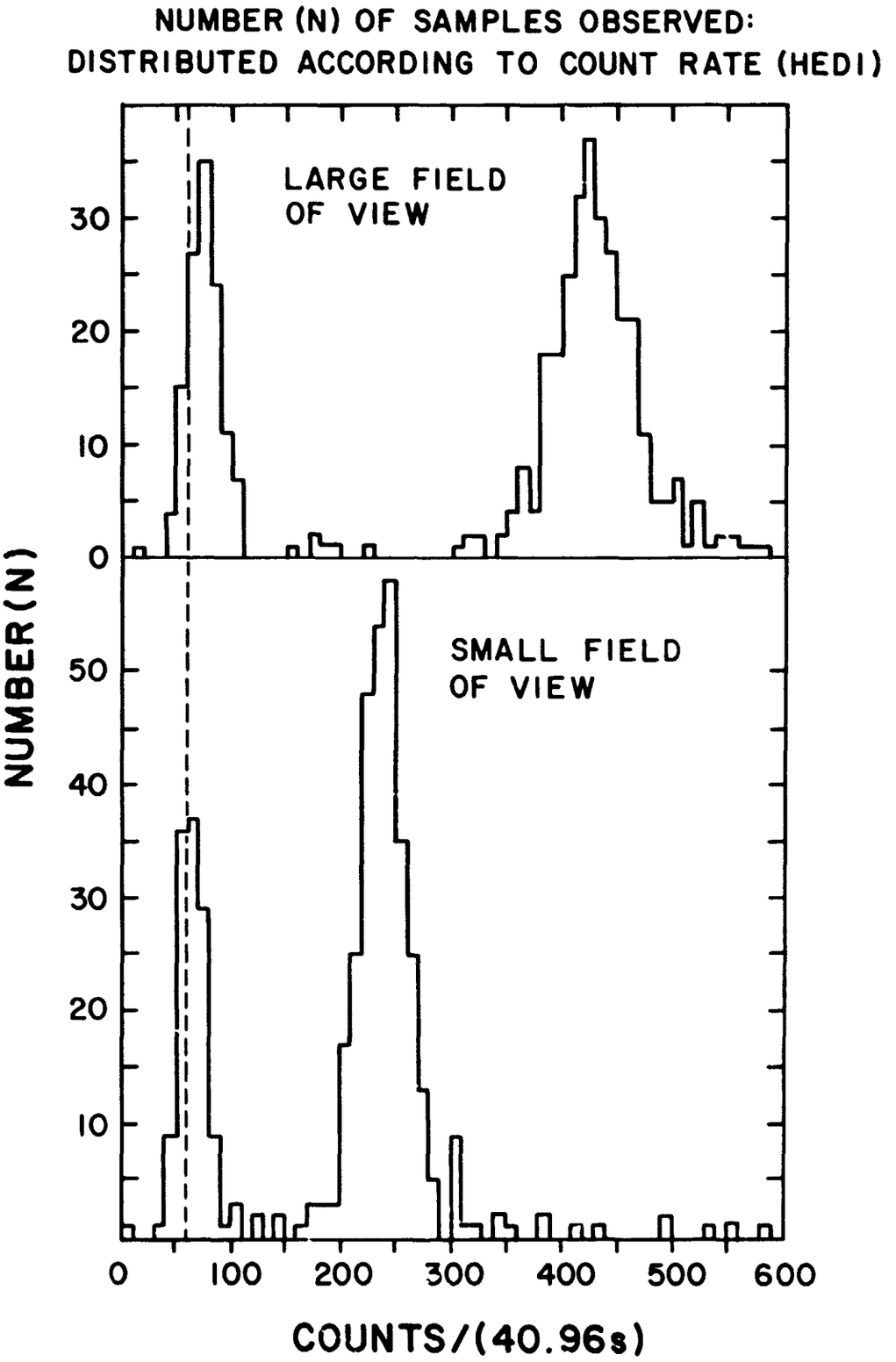
NUMBER (N) OF SAMPLES OBSERVED:
DISTRIBUTED ACCORDING TO COUNT RATE (HEDI)
LARGE FIELD
OF VIEW
SMALL FIELD
OF VIEW
NUMBER (N)
0
10
20
30
40
50
0
100
200
300
400
500
600
COUNTS/(40.96s)

FIGURE 6

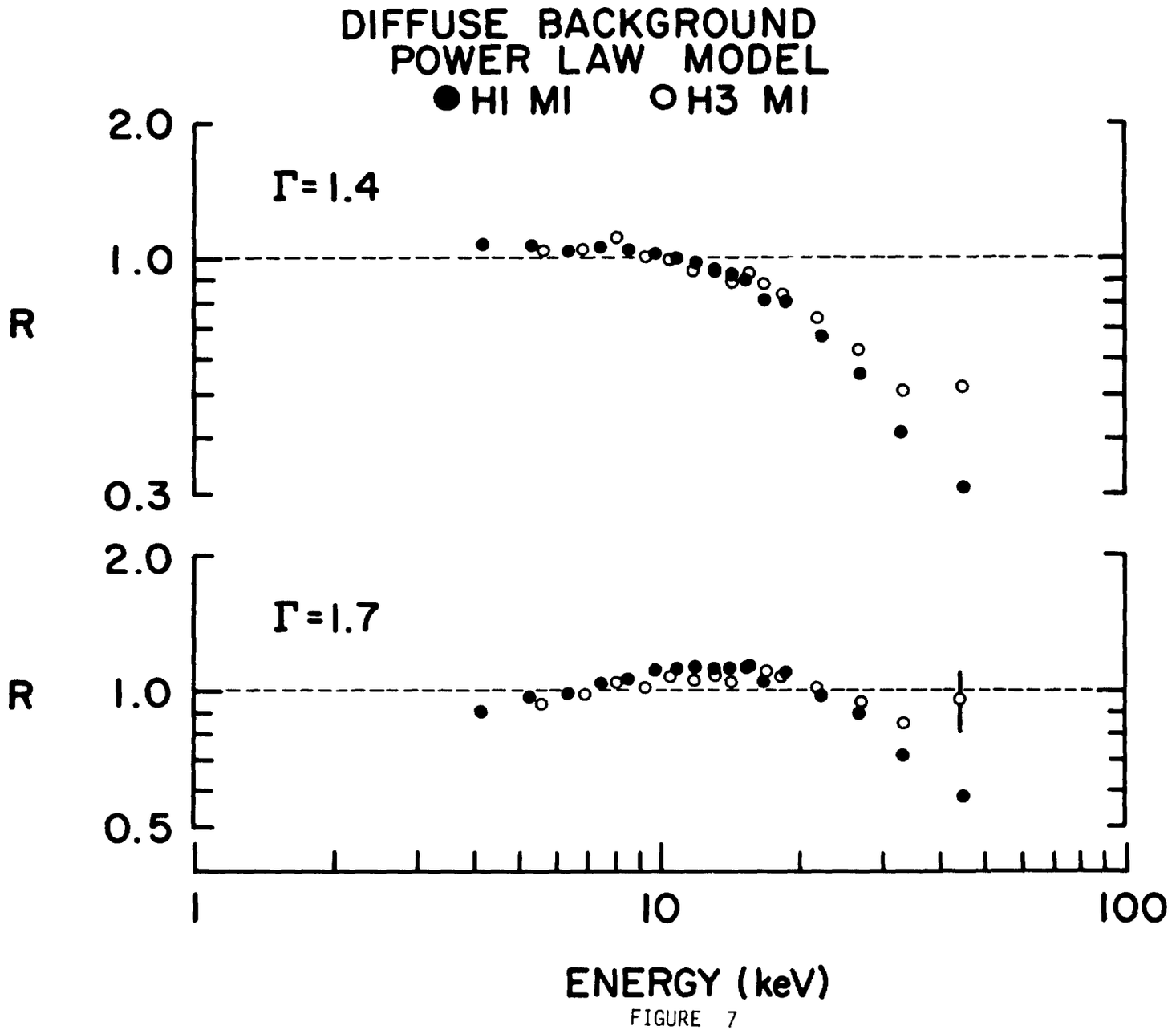
DIFFUSE BACKGROUND
POWER LAW MODEL
● H1 M1 ○ H3 M1
2.0
Γ = 1.4
1.0
R
0.3
2.0
Γ = 1.7
R
1.0
0.5
1
10
100
ENERGY (keV)

FIGURE 7

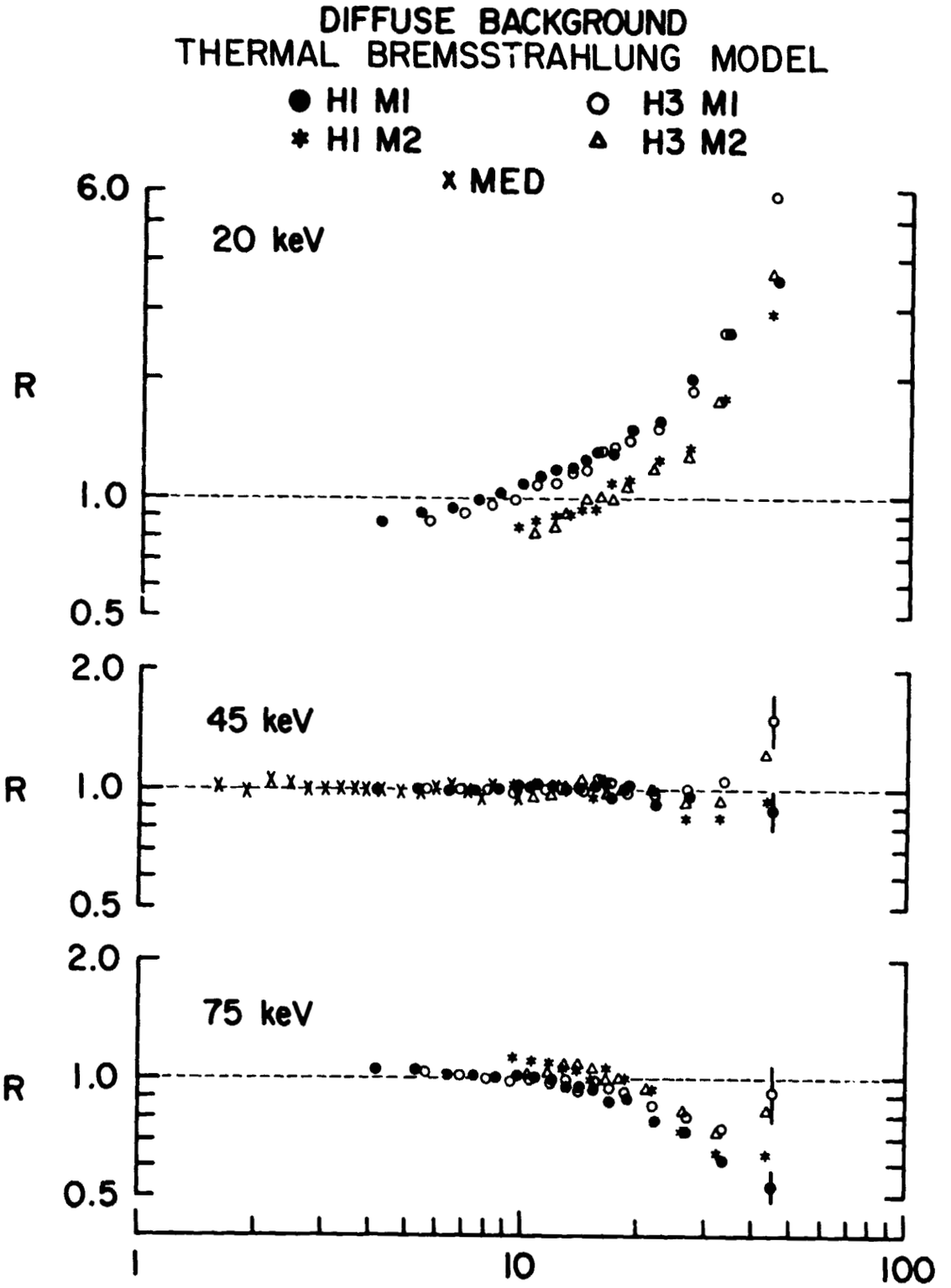

FIGURE 8

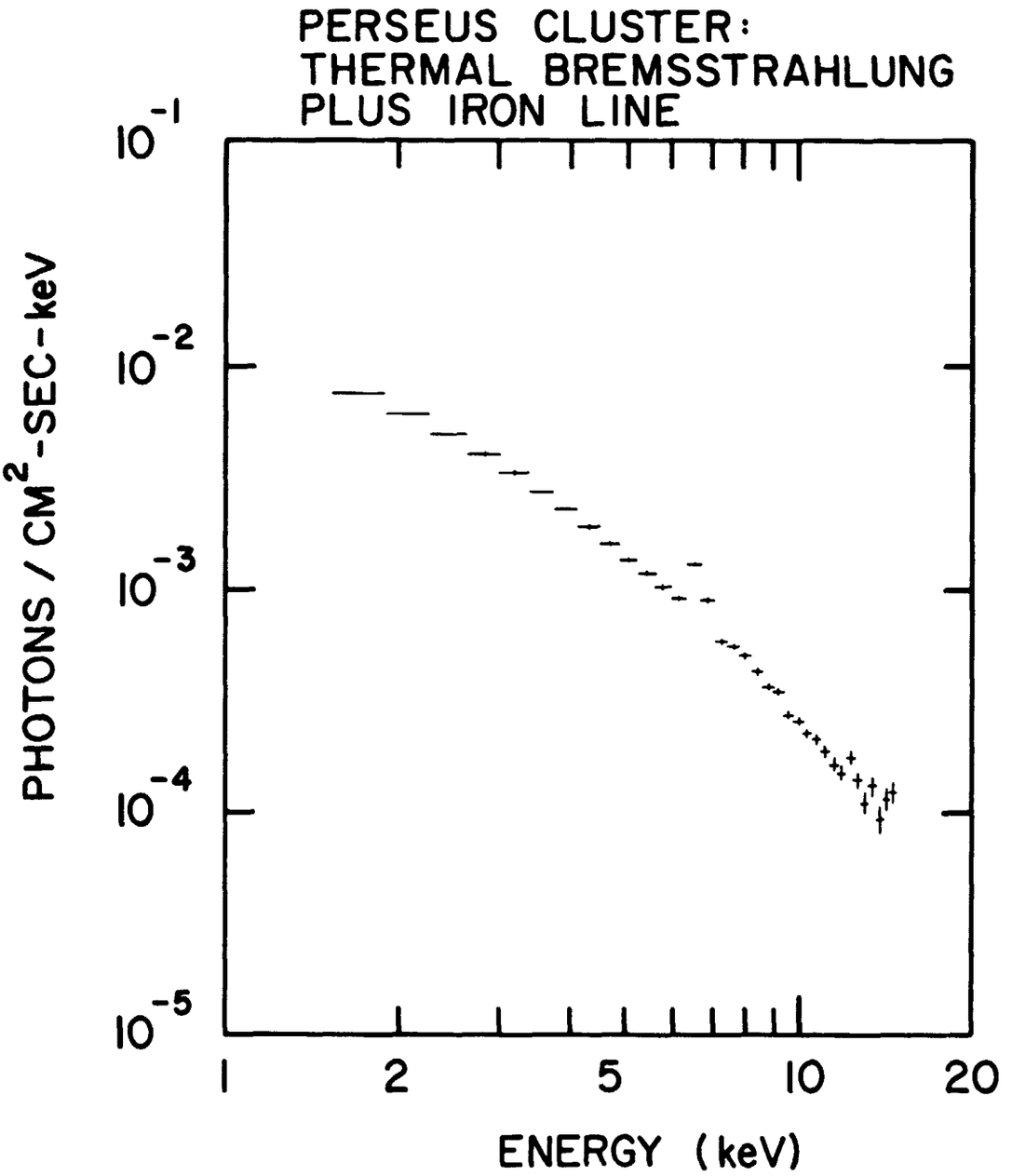
PERSEUS CLUSTER:
THERMAL BREMSSTRAHLUNG
PLUS IRON LINE
PHOTONS / CM^2-SEC-keV
10^{-1}
10^{-2}
10^{-3}
10^{-4}
10^{-5}
1
2
5
10
20
ENERGY (keV)

FIGURE 9

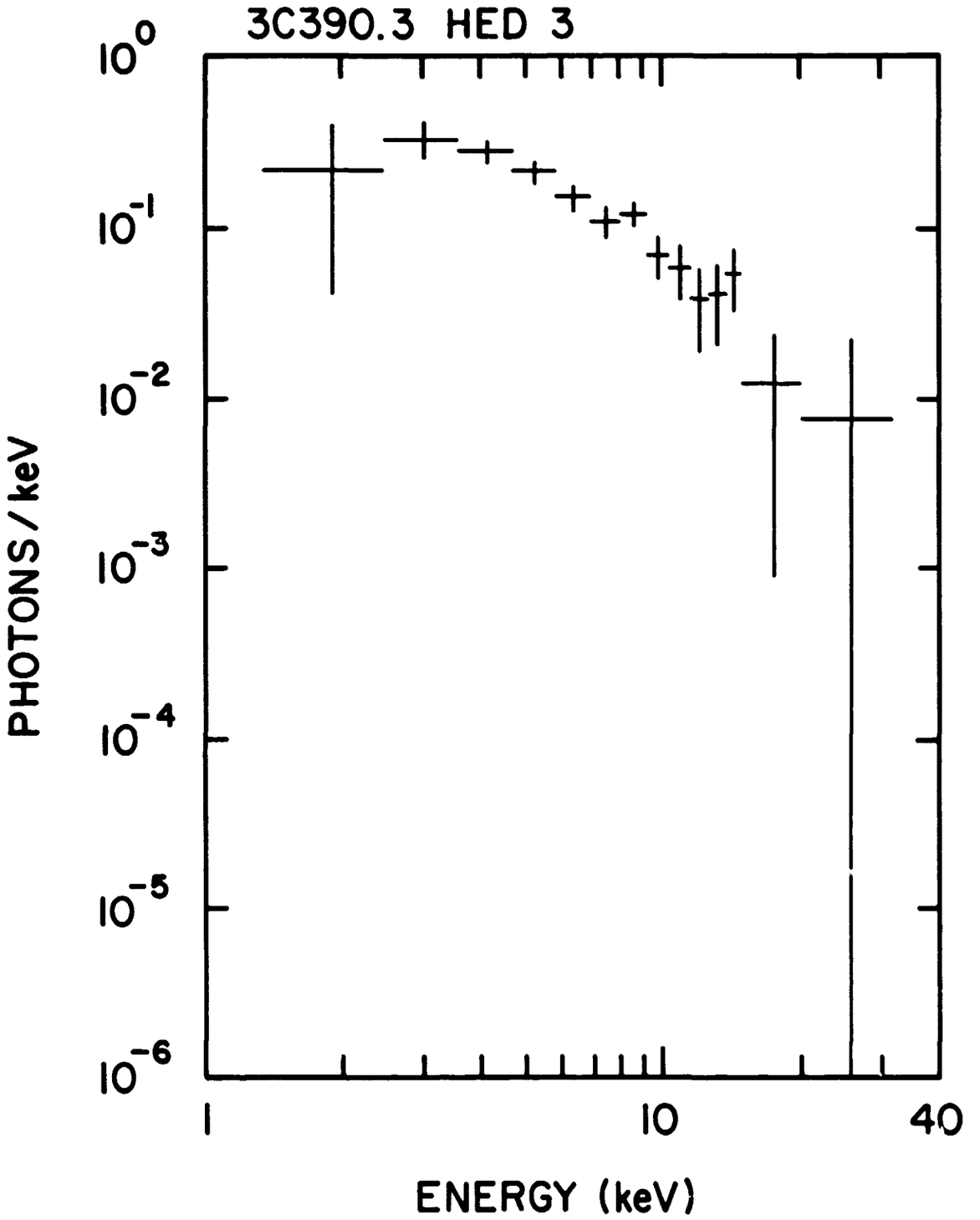
3C390.3 HED 3
10^{0}
10^{-1}
10^{-2}
10^{-3}
10^{-4}
10^{-5}
10^{-6}
PHOTONS / keV
1
10
40
ENERGY (keV)

FIGURE 10

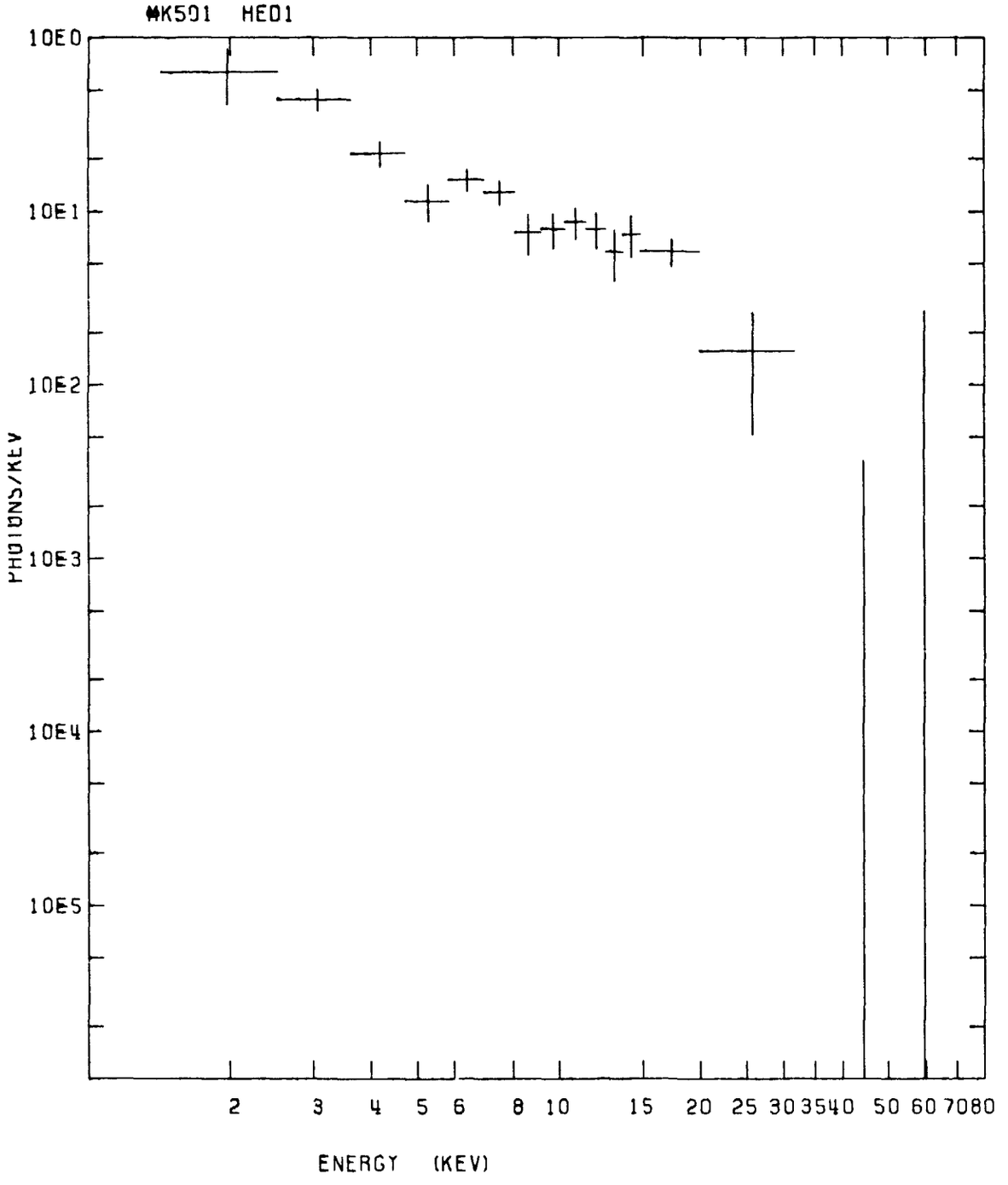

FIGURE 11

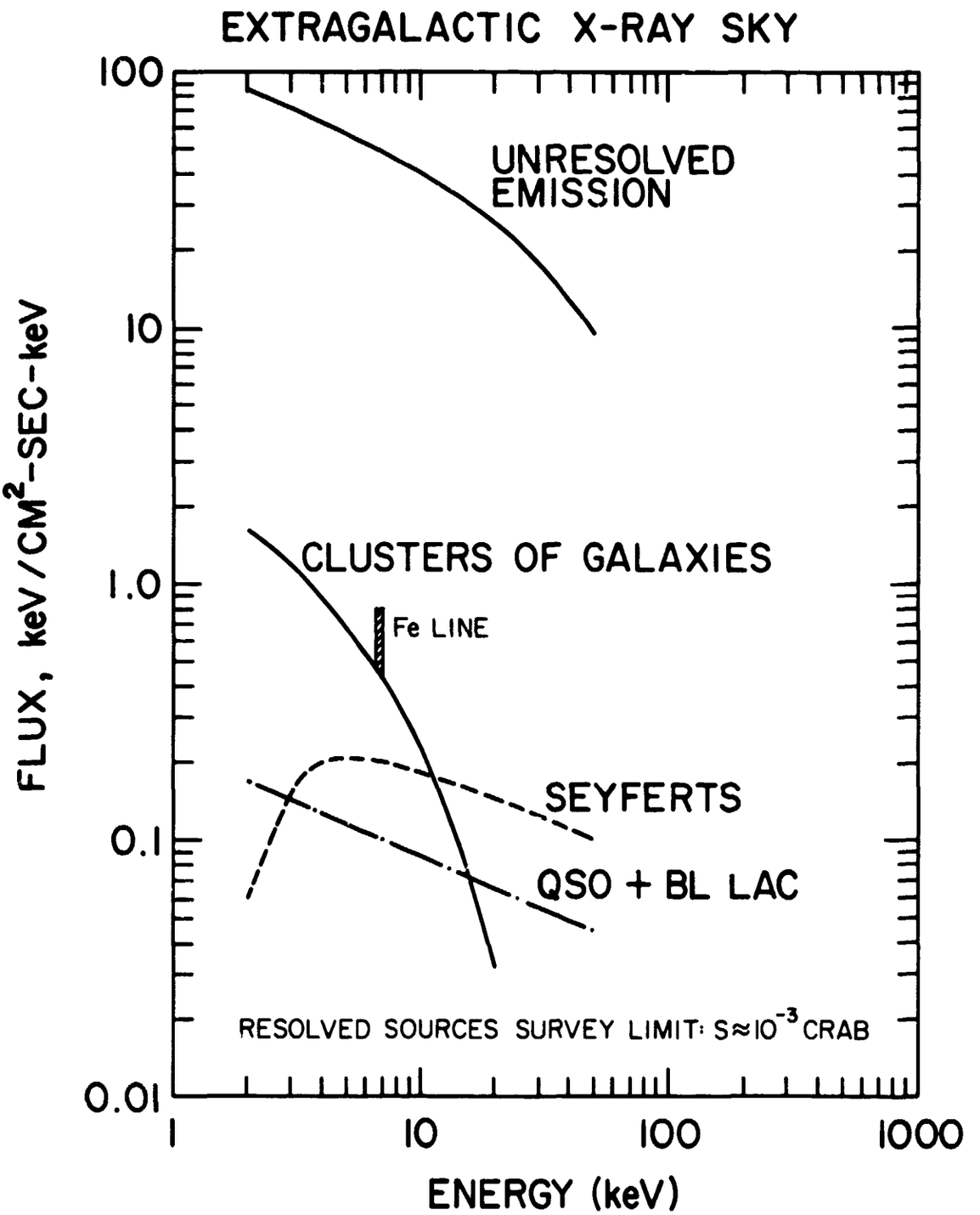
EXTRAGALACTIC X-RAY SKY
100
10
1.0
0.1
0.01
FLUX, keV/CM²-SEC-keV
UNRESOLVED EMISSION
CLUSTERS OF GALAXIES
Fe LINE
SEYFERTS
QSO + BL LAC
RESOLVED SOURCES SURVEY LIMIT: S≈10⁻³ CRAB
1
10
100
1000
ENERGY (keV)

FIGURE 12

BIBLIOGRAPHIC DATA SHEET

1. Report No.	2. Government Accession No.	3. Recipient's Catalog No.
TM 78106		

4. Title and Subtitle	5. Report Date
The Diffuse Component of the Cosmic X-Radiation	March 1978
	6. Performing Organization Code: 661

7. Author(s)	8. Performing Organization Report No.
E. A. Boldt	

9. Performing Organization Name and Address	10. Work Unit No.
Code 661 Cosmic Radiations Branch Laboratory for High Energy Astrophysics	11. Contract or Grant No.
	13. Type of Report and Period Covered: TM
12. Sponsoring Agency Name and Address	14. Sponsoring Agency Code

15. Supplementary Notes

A transcription of a talk presented in the session "First Results From HEAO-1" at the Annual Meeting of the American Association for the Advancement of Science, Washington, D. C. February 13, 1978.

16. Abstract

The A-2 experiment* on HEAO-1 is the first specifically developed to study the diffuse radiation of the entire X-ray sky over a wide bandwidth, covering both the soft X-ray emission from nearby regions of the galaxy and the isotropic hard X-radiation indicative of remote extragalactic origins. A picture that is emerging from this study is that a hot thermal plasma, on a scale comparable to that of the universe, may be the principal source of hard X-radiation characteristic of the extragalactic sky. Defining some key features of this background is a prime goal of this experiment, and work in progress on this is described.

*Principal investigators are E. Boldt, NASA/Goddard Space Flight Center, Greenbelt, Maryland and G. Garmire, California Institute of Technology, Pasadena, California.

17. Key Words (Selected by Author(s))	18. Distribution Statement
extragalactic sources--X-rays background--X-rays, spectra	

19. Security Classif. (of this report)	20. Security Classif. (of this page)	21. No. of Pages	22. Price*
U	U	38	

*For sale by the National Technical Information Service, Springfield, Virginia 22151.